

## Potentialities of $La_{0.7}Sr_{0.3}MnO_3$ thin films for magnetic and temperature sensors at room temperature

Sheng Wu<sup>\*†‡§</sup>, Dalal Fadil<sup>\*†‡§</sup>, Shuang Liu<sup>\*†‡§</sup>, Ammar Aryan<sup>\*†‡§</sup>, Benoit Renault<sup>\*†‡</sup>  
 Jean-Marc Routoure<sup>\*†‡§</sup>, Bruno Guillet<sup>\*†‡§</sup>, Stéphane Flament<sup>†‡§</sup>, Pierre Langlois<sup>\*†‡§</sup>, and Laurence Méchin<sup>\*†‡§||</sup>

<sup>\*</sup> *Université de Caen Basse-Normandie, UMR 6072 GREYC, F-14032 Caen, France.*

<sup>†</sup> *ENSICAEN, UMR 6072 GREYC, F-14050 Caen, France*

<sup>‡</sup> *CNRS, UMR 6072 GREYC, F-14032 Caen, France*

<sup>§</sup> *email addresses: first-name.name@unicaen.fr*

<sup>||</sup> *corresponding author: laurence.mechin@ensicaen.fr*

**Abstract**—In this paper, the potentialities of the manganese oxide compound  $La_{0.7}Sr_{0.3}MnO_3$  (LSMO) for the realization of sensitive room temperature thermometers and magnetic sensors are discussed. For these two applications, the sensor performances are described in terms of signal to noise ratio especially in the 1 Hz-100 kHz frequency range. It is shown that due to the very low 1/f noise level, LSMO based sensors can exhibit competitive performances at room temperature.

**Keywords**- low frequency noise, magnetoresistance sensors, thermometers

### I. INTRODUCTION

Because of the colossal magnetoresistance effect and the strong spin polarization at the Fermi level, the rare-earth manganese oxides may find important applications in magnetoresistive devices such as magnetic random access memories and magnetic sensors [1]. The large change of their electrical resistance  $R$  at the metal-to-insulator transition, which takes place around 300 K makes them potential materials for the fabrication of room temperature thermometers. Ideal materials would indeed present at the desired operating temperature  $T$  close to 300 K: i) the highest-temperature coefficient of the resistance ( $\beta_T$ ), expressed in  $K^{-1}$  and defined as the relative derivative of the resistance versus temperature  $\frac{1}{R} \cdot \frac{dR}{dT}$ , or  $\beta_H$ , expressed in  $T^{-1}$ , the highest relative change of the resistance with the magnetic field  $\mu_0 H$  and defined as  $\frac{1}{R} \cdot \frac{dR}{d(\mu_0 H)}$  (with  $\mu_0$  the vacuum permeability) and ii) the lowest noise level. The limits of the device performances will then be given by the signal to noise ratio.

Temperature coefficient of the resistance values and operating temperatures are important parameters to be considered in the fabrication of high sensitivity room-temperature thermometers or magnetoresistances. However, more attention should be drawn to the low-frequency noise level in these materials since it can vary by several orders of magnitude while  $\beta_H$  or  $\beta_T$  values may only vary by a factor less than 10. Noise is more difficult to optimize since its origin is still not well known [2].

Even if it does not exhibit the highest  $\beta_T$  or  $\beta_H$  values,  $La_{0.7}Sr_{0.3}MnO_3$  (LSMO) has been selected among all the possible manganite composition because it has shown the lowest reported low-frequency noise level so far [3]–[9].

In this paper, sample preparation is shown in the next Section. In Section III, the measurement set-up and the measurement protocol and low frequency noise measurements are presented. A discussion about the sensor performances as a function of the geometry, of the bias condition and of the frequency is given in Section IV. The performances in terms of thermometers as well as magnetoresistive sensors are then presented and compared with published values.

### II. SAMPLE PREPARATION

The sensors consist in  $t=100$  nm thick LSMO thin films deposited by pulsed laser deposition from a stoichiometric target onto  $SrTiO_3$  [001] single crystal substrate. The laser radiation energy density, the target-to-substrate distance, the oxygen pressure and the substrate temperature were 220 mJ, 50 mm, 0.35 mTorr and 720 °C respectively. These parameter values were found optimal for producing single-crystalline films with smooth surface as judged by x-ray diffraction and atomic force microscopy. The x-ray diffraction study indicated a full [001] orientation of the LSMO films. The magnetic moment as a function of the temperature was measured using a superconducting quantum interference device. We thus measured a Curie temperature of about 340 K, typical for good quality films of this composition.

After LSMO deposition, a 200 nm thick gold layer was sputtered on the films in order to make low resistive connections. The LSMO thin films were patterned by UV photolithography and argon ion etching to form lines. As shown in Figure 1, the mask enables the study of lines of four different widths  $W=20, 50, 100$  and  $150 \mu m$ . For each width, five lengths  $L$  could be measured depending on the position of the voltage contacts 50, 100, 150, 200, and  $300 \mu m$ . tens of samples with different geometries have

been investigated. Typical results for a 100 nm thick sample are reported here.

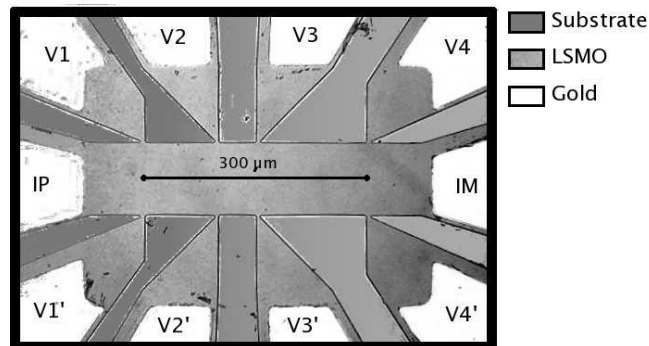


Figure 1. Optical photography of a 100  $\mu\text{m}$  width line with the two current probes IP and IM and 4 voltage probes (V1...V4, V1'...V4') on each side of the line. The line lengths between V1 -V2, V2 - V3 and V3 -V4 are 100  $\mu\text{m}$ , 50  $\mu\text{m}$  and 150  $\mu\text{m}$  respectively.

### III. LOW FREQUENCY NOISE MEASUREMENTS

#### A. Measurement set-up and protocol

The experimental set-up mainly consists in one low noise high output impedance DC current source and a dedicated low noise instrumentation amplifier with the following characteristics: a DC output dedicated to resistance measurement with a voltage gain equal to 10 and an AC output dedicated to noise measurements with a voltage gain around one thousand and a 1 Hz-1 MHz bandwidth [10]. The input voltage white noise is around  $20 \cdot 10^{-18} \text{ V}^2 \cdot \text{Hz}^{-1}$  and its input current noise is negligible. The device is connected at the output of the DC current source using IP and IM pads (defined in Figure 1). The DC voltage as well as the voltage noise are measured using the instrumentation amplifier connected either on IP, IM pads for two probe configuration or on  $V_i, V_j$  ( $i, j=1..4$  with  $i \neq j$ ) for four probe configuration. A spectrum analyzer Agilent 89410A calculates the noise spectral density for frequencies in the 1 Hz-1 MHz range.

According to [10], the DC current source is quasi-ideal: its output impedance is infinite and its noise contribution is negligible. It is also assumed that the input impedance of the instrumentation amplifier is very high so that no DC current flows in its inputs. It will be also considered that the noise contribution of the amplifier is known and can be subtracted from the measured noise when a device is connected at its input. The noise of the measurement set-up is deduced from the measurement performed at zero bias. This set-up contribution is then removed for all the measurement points when the current is non zero.

Different noise contributions that both generate white noise and 1/f noise have to be considered in the sensor: the voltage contact noise, the current contact noise and the

film noise. Details can be found in [11] and it can be shown that in the two probe configuration, the film and current contact noise contributions are measured. In the four probe configuration, due to the high output impedance of the DC current source, the current contact noise contribution can be completely eliminated. Since no DC current flows into the voltage contact, one would assumed that no 1/f noise exists for the voltage contact sources.

#### B. Obtained results

Figure 2 shows the noise spectral density measured in the two probe ( $S_{V_{2p}}$ ) and the four probe configurations ( $S_{V_{4p}}$ ) for the same DC current I. Two noise contributions were found: a white noise one and a 1/f noise one. The white noise level is clearly due the thermal noise contribution given by  $4 \cdot k_B \cdot T \cdot R$  ( $k_B$  is the Boltzmann constant equal to  $1.38 \cdot 10^{-23} \text{ J} \cdot \text{K}^{-1}$ ) and should not depend on the bias. The white noise level is consistent with the expected value deduced from the DC measurement of the sample resistance thus validating the thermal origin of the white noise.

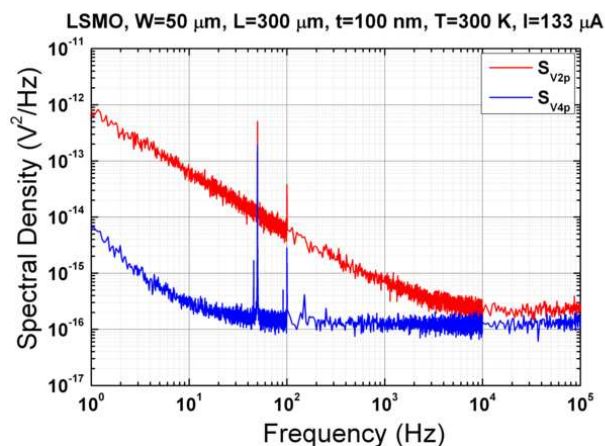


Figure 2. Noise spectral densities in the two probe ( $S_{V_{2p}}$ ) and the four probe ( $S_{V_{4p}}$ ) configurations for the same DC bias current. With the mask shown in the Figure 1, the current contact noise is non negligible and may have a great impact on sensor performances.

For this sample, the current contact contribution is much higher than the film noise. This results has already been reported by other studies [12]. It can lead to an overestimation of the film noise if the current source used for the measurement does not exhibit a large output impedance (at least 30 times higher if the current contact noise is one thousand time higher than the film noise).

The contact contribution originates from the contact between gold and LSMO and thus presents a great impact for sensor applications. The sensor can not be used with two contact configuration. A four probe configuration must be used to ensure best signal to noise ratio. Moreover, the metallic pads used for the voltage contacts have also to be

placed in a correct manner in order to avoid any possible current path through this metallic contact. As a consequence, metallic voltage pads should not be placed onto the line (like in Transmission Line Measurement (TLM) patterns for instance) but on the side of the line in order to achieve a low frequency noise level sensor.

Figure 3 shows the voltage noise spectral density measured for a typical device ( $W=50 \mu\text{m}$  and  $L=300 \mu\text{m}$ ) in four probe configuration for different values of the bias current  $I$  in the device. The inset shows the noise level at 1 Hz versus the DC voltage  $V$  across the sample. As expected, the white noise level does not depend on the bias current and  $1/f$  noise level depends on the square of the DC voltage  $V$ .

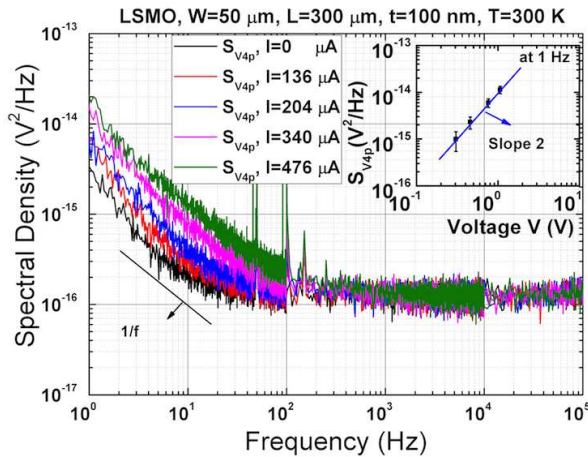


Figure 3. Noise spectral density measured in the four probe configuration at different bias currents. White noise does not depend on the bias point on the contrary of  $1/f$  noise. The inset shows that the  $1/f$  noise at 1 Hz depends on the square of the DC voltage  $V$ .

From measurements performed on different geometries, it follows that the  $1/f$  noise level at 1 Hz is in the inverse ratio of the device volume  $W \cdot L \cdot t$ . Finally, the noise spectral density of the sample in the four probe configuration  $S_{V4p}(f)$  can be written as follow:

$$S_{V4p}(f) = \frac{K_{1/f}}{f \cdot W \cdot L \cdot t} V^2 + \frac{4 \cdot k_B \cdot T \cdot \rho \cdot L}{W \cdot t} \quad (1)$$

In equation 1,  $\rho$  is the film electrical resistivity (typical value of  $2 \text{ m}\Omega \cdot \text{cm}$  for LSMO at 300 K) and  $K_{1/f}$  is a material characteristic independent of the geometry that quantify the value of the  $1/f$  noise level. In this sample,  $K_{1/f}$  is found around  $1 \cdot 10^{-30} \text{ m}^3$ .

Equation (1) clearly shows length and bias dependency of the noise are completely different in the low frequency and white noise ranges. These discussions are extended in the next Section in the framework of sensor performance analysis.

#### IV. SENSOR PERFORMANCES

In this Section, the performances in terms of signal to noise ratio will be presented and discussed in the case of thermometers and magnetoresistance sensors.

##### A. Background

To use the devices as sensors, a current source is connected and the voltage across the sensor is measured. A four probe configuration will be used to avoid the current contact noise contribution. Either the temperature  $T$  or the magnetic field  $\mu_0 H$  are the mesurand. For these theoretical derivations, the mesurand will be noted  $M$  and the relative sensitivity  $\beta_M$ , defined in the following equation, will be used:

$$\beta_M = \frac{1}{R} \cdot \left( \frac{dR}{dM} \right)_{M0} \quad (2)$$

$M0$  is the DC value of the mesurand for which the relative sensitivity is estimated. The equivalent input sensor noise  $S_M(f)$  is given by the ratio of the voltage noise spectral density of the sensor  $S_V(f)$  (given by  $S_{V4p}(f)$  in the case of our LSMO samples in the previous sample) over the square of the voltage sensitivity at  $M0$  given by  $(dV/dM = V \cdot \beta_M)$ . Using equation (1), it follows that  $S_M(f)$  finally writes:

$$\begin{aligned} S_M(f) &= \frac{S_V(f)}{(dV/dM)^2} \\ &= \frac{1}{\beta_M^2} \left( \frac{K_{1/f}}{f \cdot W \cdot L \cdot t} + \frac{4 \cdot k_B \cdot T \cdot \rho \cdot L}{V^2 \cdot t \cdot W} \right) \end{aligned} \quad (3)$$

In order to obtain the smallest noise sensor, this equation shows that in addition to large sensitivity values, low value of the  $1/f$  noise parameter  $K_{1/f}$  and low value of the electrical resistivity are first required. Two geometrical and bias dependencies can then be distinguished:

- in the low frequency part where  $1/f$  noise dominates, the equivalent input sensor noise does not depend on the bias and the sample should have the largest volume  $W \cdot L \cdot t$ .
- in the white noise range of frequencies, the equivalent input sensor noise decreases with the square of the bias voltage. The geometry should have the smallest ratio value  $L/W$  and the sensor should also be as thick as possible.

All these considerations obviously do not take into account other constraints such as frequency bandwidth or cost, which usually leads to opposite conclusions in term of device volume or size. These results are illustrated in the next Sections for thermometers and magnetoresistance sensors for a optimal devices regards  $1/f$  noise ( $L=300 \mu\text{m}$ ,  $W=150 \mu\text{m}$ ).

**B. Thermometers**

LSMO electrical resistivity  $\rho$  and relative temperature sensitivity  $\beta_T$  (also called TCR for thermometers) versus temperature  $T$  are shown in Figure (4). In this kind of material, a transition from metallic to insulator behavior occurs for temperature close to room temperature as already reported [13]. In this sample, the maximum value of  $\beta_T$  is found for temperature close to 330 K. A typical value is reported in Table I.

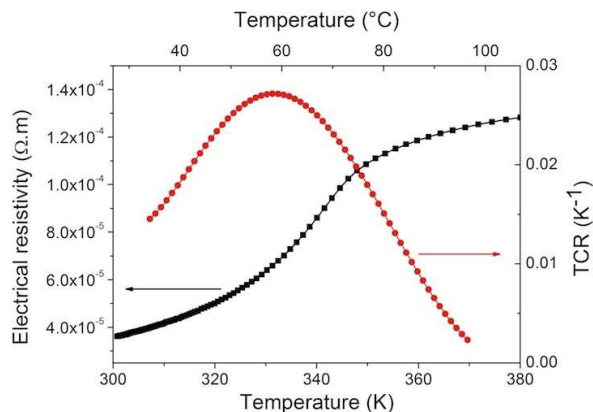


Figure 4. LSMO electrical resistivity  $\rho$ (square symbols, left axis) and relative temperature sensitivity  $\beta_T$  (circle symbols, right axis) versus temperature  $T$  in the 300-380 K range for a line with  $W=50 \mu\text{m}$  and  $L=300 \mu\text{m}$ . The maximum sensitivity is found around 330 K where  $\beta_T=2.7 \cdot 10^{-2} \text{ K}^{-1}$ .

**C. Magnetoresistance sensors**

LSMO electrical resistance and relative magnetic field sensitivity  $\beta_H$  as a function of the magnetic field  $\mu_0 \cdot H$  are shown in the Figure 5. Due to the ferromagnetic behavior of LSMO at room temperature, a magnetoresistance effect is observed. Two kinds of effect can be distinguished: i) a Colossal MagnetoResistance effect (CMR) for magnetic field values greater than 2 mT [14], [15] and ii) a low magnetoresistance effect for magnetic field values close to 0.5 mT. The first one leads to a small sensitivity with no interesting sensor applications. The second one is related to the magnetization reversal [16]–[18]. It leads to two peaks in the  $R$  versus  $\mu_0 H$  characteristic and a relatively high value of the relative magnetic field sensitivity (absolute typical values around  $1 \text{ T}^{-1}$  for an operation point around  $1 \text{ mT}$ ) at room temperature (cf. Table I).

**D. Discussions**

In this discussion, it will be assumed that the thermometer or the magnetoresistance is connected in four probe configuration and that the device geometry leads to the smallest value of  $1/f$  noise. The noise performances in terms of equivalent input sensor noise values of DC current will be

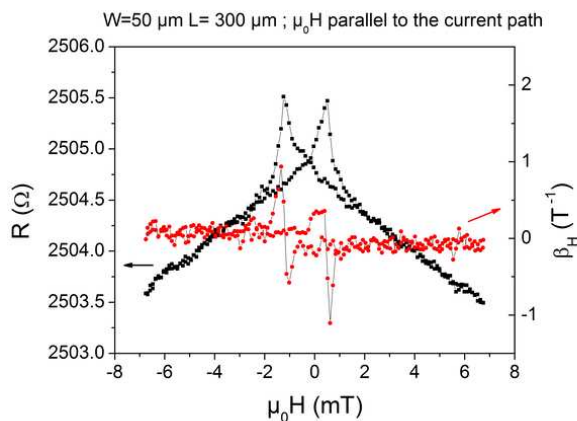


Figure 5. LSMO electrical resistance  $R$  (square symbols, left axis) and relative magnetic field sensitivity  $\beta_H$  (circle symbols, right axis) as a function of the magnetic field  $\mu_0 \cdot H$  at room temperature for a line with  $W=50 \mu\text{m}$  and  $L=300 \mu\text{m}$ . Magnetic field is parallel to the current direction. Sensitivity maxima observed at low magnetic field are related to the magnetization reversal in the film.

Parameter	Value
$K_{1/f}$ ( $\text{m}^3$ ) at 300 K	$1 \cdot 10^{-30}$
$\rho$ ( $\Omega \cdot \text{m}$ ) at 300 K, at 330 K	$3.5 \cdot 10^{-5}$ , $6.3 \cdot 10^{-5}$
$\beta_T$ at 330 K ( $\text{K}^{-1}$ )	$2.7 \cdot 10^{-2}$
$\beta_{HMAX}$ at 300 K ( $\text{T}^{-1}$ )	$\simeq 1$

Table I  
TYPICAL ELECTRICAL CHARACTERISTICS AND NOISE PROPERTIES OF THE SAMPLE USED FOR THE ESTIMATIONS OF THE SIGNAL TO NOISE RATIO. FOR THESE VALUES, THE DEVICE LENGTH AND WIDTH ARE RESPECTIVELY  $300 \mu\text{m}$  AND  $50 \mu\text{m}$ .

calculated with the data in Table I for three values of the DC current  $I=100 \mu\text{A}$ ,  $I=1 \text{ mA}$  and  $I=5 \text{ mA}$ .

Table II summarizes the results for a  $150 \mu\text{m}$  wide and  $300 \mu\text{m}$  long thermometer or magnetoresistance at optimal operating point (330 K for the thermometer, 300 K and 0.1 mT for the magnetoresistance). In this Table, the equivalent input sensor noise has been calculated at two frequencies (30 Hz and 10 kHz) to distinguish between the low frequency domain where  $1/f$  noise dominates and the white noise domain.

The equivalent input sensor spectral densities  $S_T(f)$  (also called NET Noise Equivalent Temperature) and  $S_H(f)$  calculated using equation 3 and data from Table I are shown in Figure 6. As expected, the spectral density at low frequency does not depend on the bias when  $1/f$  noise dominates. On the contrary, at high frequency, the noise level is directly related to the applied bias current. From this Figure, it appears that ultimate performances can be achieved at highest current. This remarks has obviously to be moderated by the fact that self heating effects occur for too high current values so that the noise performances will

Bias current $I$ (mA)	0.1	1	5
$\frac{dV}{d(\mu_0 H)}$ at 300 K (mV/T) (*)	45.5	455	2275
$\sqrt{S_H(f)}$ at 300 K (nT·Hz <sup>-0.5</sup> )			
f=30 Hz	78	8.6	4.4
f=10 kHz	75	7.5	1
$\frac{dV}{dT}$ at 330 K (mV/K) (**)	3.4	34	170
$\sqrt{S_T(f)}$ at 330 K (nK·Hz <sup>-0.5</sup> )			
f=30 Hz	1400	170	100
f=10 kHz	1400	140	30

Table II

SENSOR PERFORMANCES FOR A 150  $\mu\text{m}$  WIDE 300  $\mu\text{m}$  LONG LINE AT DIFFERENT BIAS CURRENT  $I$ . (\*  $R=700 \Omega$  at 300 K, \*\*  $R=1260 \Omega$  at 330 K.)

be discussed in the following for a bias current limited to 100  $\mu\text{A}$ . At low bias current, the 1/f noise contribution is negligible. In this LSMO sample, due to the low value of the 1/f noise level, the noise spectral density mainly consists in white noise even at a bias current of about 300  $\mu\text{A}$ .

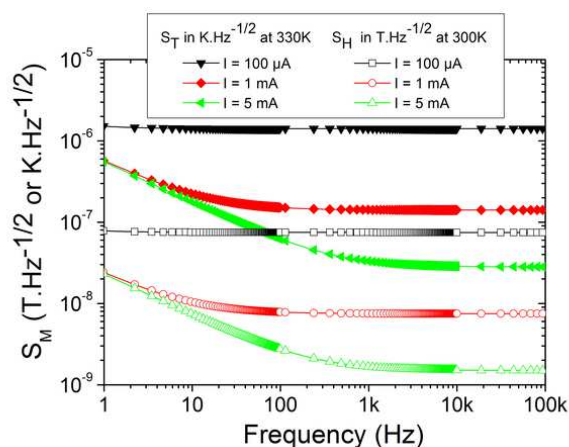


Figure 6. Square root of the estimated equivalent input sensor spectral densities  $S_T(f)$  (filled symbols) or  $S_H(f)$  (open symbols) using equation (3) and the Table I data for three values of the DC current  $I$  for a 150  $\mu\text{m}$  width and 300  $\mu\text{m}$  length sensor.

These NET values are lower (at least one magnitude order) than the one of other uncooled thermometers such as amorphous semiconductors, vanadium oxides, etc. or the well-known Pt100 thermometer [8], [9]. This can easily be explained by the lower noise level of epitaxial manganites thin films compared to others. The results show that despite a quite small TCR value and thanks to a very low-noise level, LSMO thin films are real potential material for uncooled thermometry.

According to [19] where equivalent input sensor spectral densities  $S_H(f)$  have been compared for various kinds of magnetic sensors, this LSMO magnetoresistance noise performances are better than hall effect sensors. Equivalent input sensor spectral densities is only one order of magnitude

higher than commercial honeywell HMC1001 sensors. Same results are also proposed by [19], [20]. These results are promising since the mask used was not optimized for sensor applications so that the sensitivity could be increased by changing the substrate type or the line geometry. Moreover, it has been demonstrated that LSMO can be deposited onto silicon substrate [21] without modifications of the magnetic properties: compatibility with the standard semiconductor used in the microelectronic industry has thus been demonstrated. This is another way to extend to "More than Moore" idea proposed by the International Roadmap for Semiconductor by the integration of manganese oxide.

### V. CONCLUSIONS

In this paper, the potentialities of LSMO thin films as magnetic and temperature sensors at room temperature have been reported. It has been shown that a four probe configuration is required to remove the current contact noise that is often several order of magnitude higher than the material noise. In such conditions, It has been shown that the performances of the room thermometers are competitive and that magnetoresistance exhibits noise performances one decade better than classical hall effect sensors.

### REFERENCES

- [1] T. Venkatesan, M. Rajeswari, Z.-W. Dong, S. B. Ogale, and R. Ramesh, "Manganite-based devices: opportunities, bottlenecks and challenges," *Philos. Trans. R. Soc. London, Ser. A*, vol. 356, no. 1742, pp. 1661–1680, 1998.
- [2] M. Rajeswari, A. Goyal, A. Raychaudhuri, M. Robson, G. Xiong, C. Kwon, R. Ramesh, R. Greene, T. Venkatesan, and S. Lakeou, "1/f electrical noise in epitaxial thin films of the manganite oxides  $\text{La}_{0.67}\text{Ca}_{0.33}\text{MnO}_3$  and  $\text{Pr}_{0.67}\text{Sr}_{0.33}\text{MnO}_3$ ," *Appl. Phys. Lett.*, vol. 69, no. 6, pp. 851–853, 1996.
- [3] B. Raquet, J. Coey, S. Wirth, and S. von Molnár, "1/f noise in the half-metallic oxides  $\text{CrO}_2$ ,  $\text{Fe}_3\text{O}_4$ , and  $\text{La}_{2/3}\text{Sr}_{1/3}\text{MnO}_3$ ," *Phys. Rev. B*, vol. 59, no. 19, pp. 12435–12443, 1999.
- [4] A. Lisauskas, S. Khartsev, and A. Grishin, "Studies of 1/f Noise in  $\text{La}_{1-x}\text{M}_x\text{MnO}_3$  (M= Sr, Pb) Epitaxial Thin Films," *J. Low Temp. Phys.*, vol. 117, no. 5, pp. 1647–1651, 1999.
- [5] A. Palanisami, R. Merithew, M. Weissman, M. Warusawithana, F. Hess, and J. Eckstein, "Small conductance fluctuations in a second-order colossal magnetoresistive transition," *Phys. Rev. B*, vol. 66, no. 9, p. 92407, 2002.
- [6] L. Méchin, J.-M. Routoure, S. Mercone, F. Yang, S. Flament, and R. Chakalov, "1/f noise in patterned  $\text{La}_{0.7}\text{Sr}_{0.3}\text{MnO}_3$  thin films in the 300–400 K range," *J. Appl. Phys.*, vol. 103, p. 083709, 2008.
- [7] K. Han, Q. Huang, P. Ong, and C. Ong, "Low-frequency noise in  $\text{La}_{0.7}\text{Sr}_{0.3}\text{Mn}_{1-x}\text{F}_x\text{O}_3$  thin films," *J. Phys. Condens. Matter*, vol. 14, p. 6619, 2002.

- [8] F. Yang, L. Méchin, J.-M. Routoure, B. Guillet, and R. A. Chakalov, "Low-noise  $La_{0.7}Sr_{0.3}MnO_3$  thermometers for uncooled bolometric applications," *J. Appl. Phys.*, vol. 99, no. 2, p. 024903, Jan 2006.
- [9] L. Méchin, J.-M. Routoure, B. Guillet, F. Yang, S. Flament, D. Robbes, and R. Chakalov, "Uncooled bolometer response of a low noise  $La_{2/3}Sr_{1/3}MnO_3$  thin film," *Appl. Phys. Lett.*, vol. 87, p. 204103, 2005.
- [10] J.-M. Routoure, D. Fadil, S. Flament, and L. Méchin, "A low-noise high output impedance DC current source," in *Proceedings of the 19th International Conference on Noise and Fluctuations; ICNF 2007, AIP Conference Proceedings*, vol. 922, no. 1, 2007, pp. 419–424.
- [11] C. Barone, A. Galdi, S. Pagano, O. Quaranta, L. Méchin, J. Routoure, and P. Perna, "Experimental technique for reducing contact and background noise in voltage spectral density measurements," *Rev. Sci. Instrum.*, vol. 78, p. 093905, 2007.
- [12] C. Barone, S. Pagano, L. M. echin, J.-M. Routoure, P. Orgiani, and L. Maritato, "Apparent volume dependence of 1/f noise in thin film structures: Role of contacts," *Rev. Sci. Instrum.*, vol. 79, p. 053908, 2008.
- [13] A. Urushibara, Y. Moritomo, T. Arima, A. Asamitsu, G. Kido, and Y. Tokura, "Insulator-metal transition and giant magnetoresistance in  $La_{1-x}Sr_xMnO_3$ ," *Phys. Rev. B*, vol. 51, no. 20, pp. 14 103–14 109, 1995.
- [14] J. O'Donnell, M. Onellion, M. Rzchowski, J. Eckstein, and I. Bozovic, "Low-field magnetoresistance in tetragonal  $La_{1-x}Ca_xMnO_3$  sfilms," *Phys. Rev. B*, vol. 55, no. 9, p. 5873, 1997.
- [15] —, "Anisotropic properties of molecular beam epitaxy-grown colossal magnetoresistance manganite thin films," *J. Appl. Phys.*, vol. 81, p. 4961, 1997.
- [16] M. Saïb, M. Belmeguenai, L. Méchin, D. Bloyet, and S. Flament, "Magnetization reversal in patterned  $La_{0.67}Sr_{0.33}MnO_3$  thin films by magneto-optical Kerr imaging," *J. Appl. Phys.*, vol. 103, no. 11, p. 113905, Jun 2008.
- [17] L. Méchin, P. Perna, M. Saïb, M. Belmeguenai, S. Flament, C. Barone, J. Rouroure, and C. Simon, "Structural, 1/f noise and MOKE characterization of vicinal  $La_{0.7}Sr_{0.3}MnO_3$  thin films," *Acta Phys. Pol. A*, vol. 111, no. 1, pp. 63–70, 2007.
- [18] T. McGuire and R. Potter, "Anisotropic magnetoresistance in ferromagnetic 3d alloys," *IEEE Trans. Magn.*, vol. 11, no. 4, pp. 1018– 1038, 1975.
- [19] A. Jander, C. Smith, and R. Schneider, "Magnetoresistive sensors for nondestructive evaluation (Invited Paper)(Proceedings Paper)," in *proceeding of the 10th SPIE International Symposium, Nondestructive Evaluation for Health Monitoring and Diagnostics, Conference 5770*, Jan 2005.
- [20] M. Díaz-Michelena, "Small magnetic sensors for space applications," *Sensors*, vol. 9, no. 4, pp. 2271–2288, 2009.
- [21] M. Belmeguenai, S. Mercone, C. Adamo, L. Méchin, C. Fur, P. Monod, P. Moch, and D. G. Schlom, "Temperature dependence of magnetic properties of  $La_{0.7}Sr_{0.3}MnO_3/SrTiO_3$  thin films on silicon substrates," *Phys. Rev. B*, vol. 81, no. 5, p. 054410, Feb 2010.